Electronic Supplementary Information

Octahedral-shaped perovskite nanocrystals and their visible-light photocatalytic activity†

Simin Yin[a‡], He Tian[b‡], Zhaohui Ren[a*], Xiao Wei[ac], Chunying Chao[a], Jingyuan Pei[ac], Xiang Li[a], Gang Xu[a], Ge Shen[a], Gaorong Han[a*]

a State Key Laboratory of Silicon Materials Department of Materials Science and Engineering, Cyrus Tang Center for Sensor Materials and Application, Zhejiang University, Hangzhou P.R. China

b EMAT, University of Antwerp, Groenenborgerlaan 171, B-2020 Antwerp, Belgium

c Electron Microscope Center of Zhejiang University, Hangzhou, 310027, P. R. China

Email: renzh@zju.edu.cn; hgr@zju.edu.cn

Experimental section:

Synthesis: Single crystal perovskite $PbTiO_3$ nano-octahedra (PT OCT) were synthesized via a hydrothermal method. Briefly, 0.4g TiO_2 was dissolved in 6M KOH aqueous solution, then $Pb(NO_3)_2$ aqueous solution was dropped into it to form a suspension where Ti : Pb ratio is designed to be 1:1.25. Subsequently, $LiNO_3$ aqueous solution was added under vigorous stirring into above mixture to form hydroxide precursor. The as-prepared precursor was then transferred to a homemade Teflon-lined stainless autoclave. The feedstock volume was adjusted to 35 ml by deionized water. The autoclave was sealed, heat treated at 200 ^oC for 12 h, and then cooled to room temperature in air naturally. The resultant white powder was washed with deionized water and ethanol for several times before it is dried at 60 ^oC for 12 h for characterization.

Characterization: X-Ray powder diffraction (XRD) patterns were collected at room temperature on a RIGAKUD-MAX-C diffractometer with CuKa radiation (λ = 1.54056 Å). Scanning electron microscope (SEM) images were collected by Hitachi field emission SEM MODEL S-4800 equipped with an EDS detector. High-angle annular dark field (HAADF) scanning TEM (STEM) experiments and electron energy loss spectroscopy (EELS) studies were performed using an FEI Titan 50-80 equipped with a post-column GIF detector. The Titan was equipped with a probe corrector in STEM mode making the nominal resolution 80 pm working under 120 KeV high tensions. The UV-Vis absorption spectra were measured on a UV-VIS-NIR spectrophotometer (UV-3600 Shimadzu). The XPS spectra were investigated by an XPS device of Thermo ESCALAB 250 using a monochromatized Al Kα ($h\upsilon$ = 1486.6 eV, 150 W) exciting radiation. The electron spin resonance (ESR) measurements were performed at 300 K on an ESRA-300 Bruker spectrometer. A 100W Oriel Hg lamp was used to illuminate the sample.

Photocatalytic Experiments: The photodegradation of methylene blue (MB) dye was observed by using absorption spectroscopy. In a typical process, an aqueous solution of MB (10^{-5} M, 100 ml) and the photocatalyst (0.1 g) were placed in a 150 ml cylindrical reaction vessel. At given time intervals, the photoreacted solution was analyzed by recording variations of the absorption band maximum (664 nm) in the UV-visible spectra of MB. Under ambient conditions and continuous stirring, the photoreaction vessel was exposed to the visible-light irradiation produced by a 300 W xenon lamp equipped with a cutoff filter as the light source (λ> 420 nm). Particularly, in circle degradation process, as aqueous solution of MB (10^{-5} M, 100 ml) and the photocatalyst of 0.5g was used and the following procedure was the same.

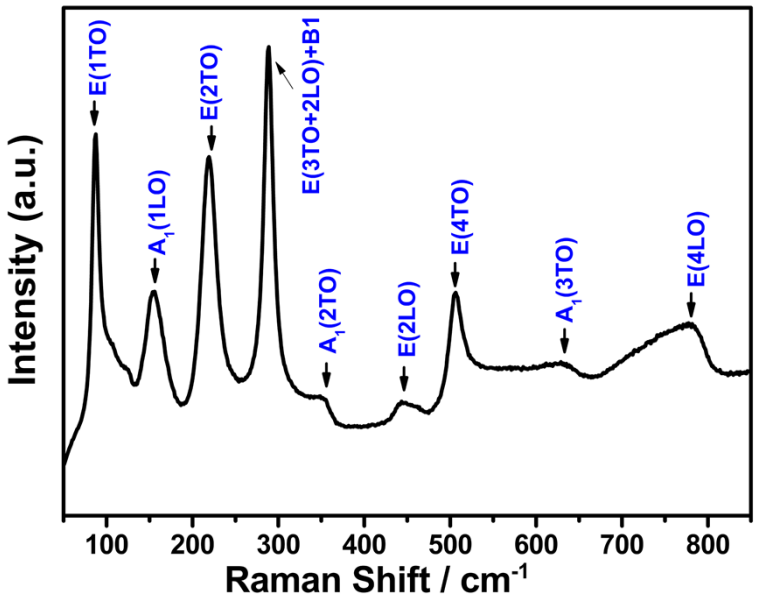

Fig.S1 Typical Raman spectrum of the as-synthesized PT OCT nanocrystals

Raman spectrum of the as-synthesized PT OCT nanocrystals was examined and shown in Fig. S1. Corresponding Raman peaks at ~ 88.2 cm^{-1}, 154.1 cm^{-1}, 220.1 cm^{-1}, 290.3 cm^{-1}, 505.7 cm^{-1}, 782.3 cm^{-1}, 356.3 cm^{-1}, 444.2 cm^{-1} and 633.0 cm^{-1}can be well assigned to different active modes of the tetragonal perovskite $PbTiO_3$.[1]

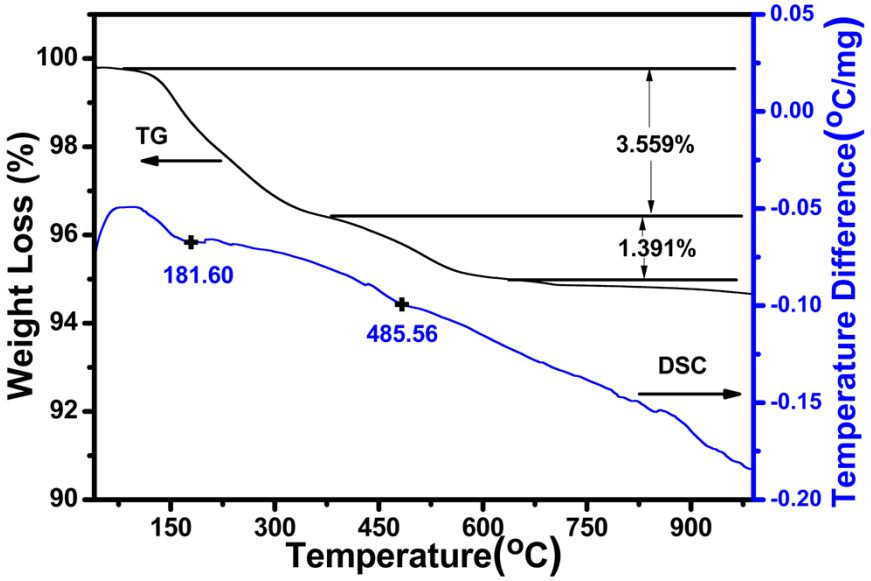

Fig.S2 TG-DSC plot of the as-synthesized PT OCT nanocrystals

Fig.S2 shows the TG-DSC analysis result of PT OCT nanocrystals. The first peak at 181.6 °C can be identified as physically absorbed water evaporation or the decomposition of intermediate products.[2]

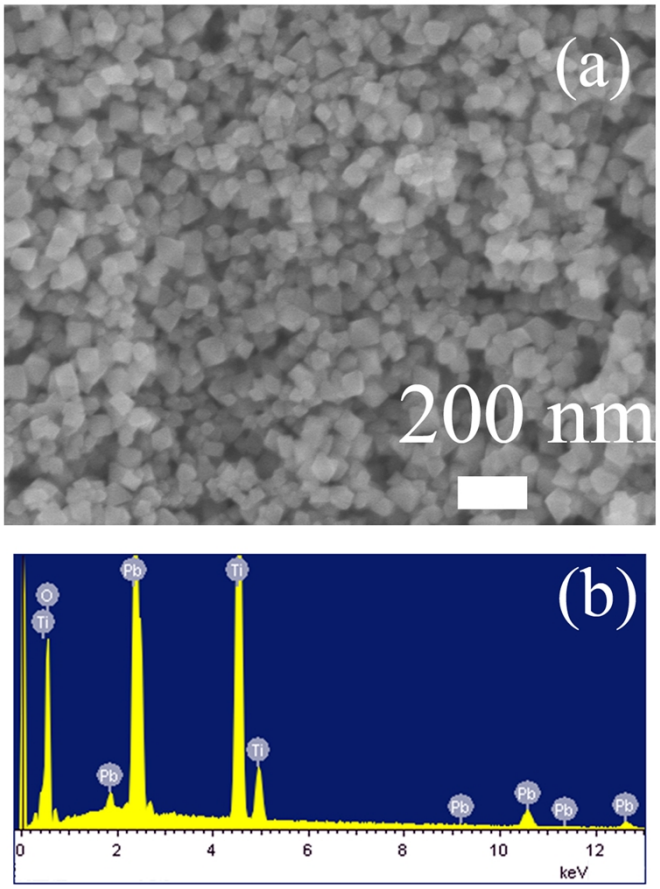

Fig.S3 (a) Low magnification SEM image and (b) energy dispersion spectroscopy (EDS) of the as-synthesized PT OCT nanocrystals

Fig.S3 gives the typical low-magnitude SEM image of as-synthesized PT OCT nanocrystals and the corresponding EDS spectrum. It can be revealed that large-scale octahedral-shaped nanocrystals with size in the range of 50-100 nm were formed, clearly containing Pb, Ti and O elements.

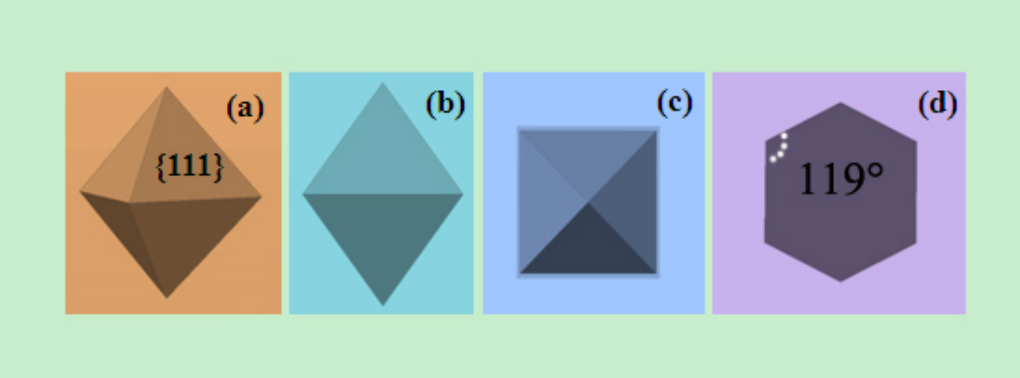

Fig.S4 (a) a simple OCT model, geometrically derived from the unit cell of tetragonal perovskite PT, and (b)-(d) the corresponding projections of the OCT along [100], [001] and [111] orientation, respectively.

Fig.S4 (a) presents a schematic illustration of a geometric model of a single tetragonal PT OCT, enclosed with {111}. Fig.S4 (b)-(d) gives the projections observed along three different orientations, respectively. The square-like geometry in Fig.S4(c) was exactly the same as observed in TEM (as in Fig.2 (e)). Specifically, the angle has been calculated to be 119°when the unit cell was observed along [111] direction, adopting a hexagon configuration as shown in Fig. 2(g) (the angle in the hexagon projection was 117°, basically the same with the value calculated here.)

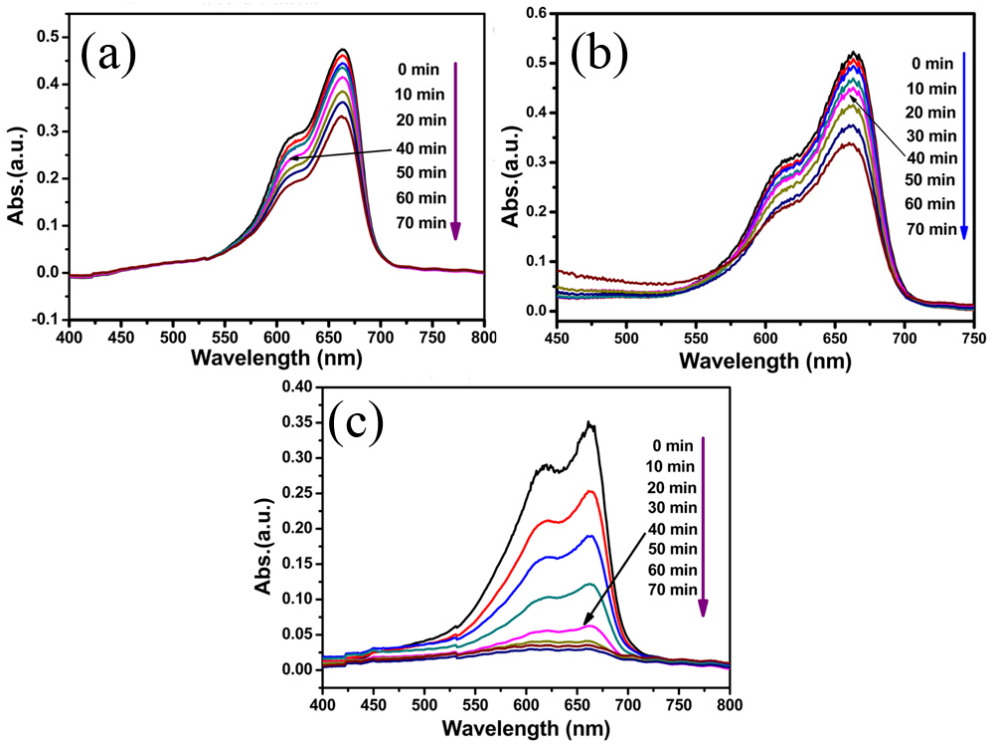

Fig.S5 Absorption changes of MB solution during photocatalytic process under visible light: (a) MB self-degradation, (b) MB degradation with the presence of P25 TiO_2 and (c) MB degradation with the presence of PT OCT (MB solution concentration is 10^{-5} M)

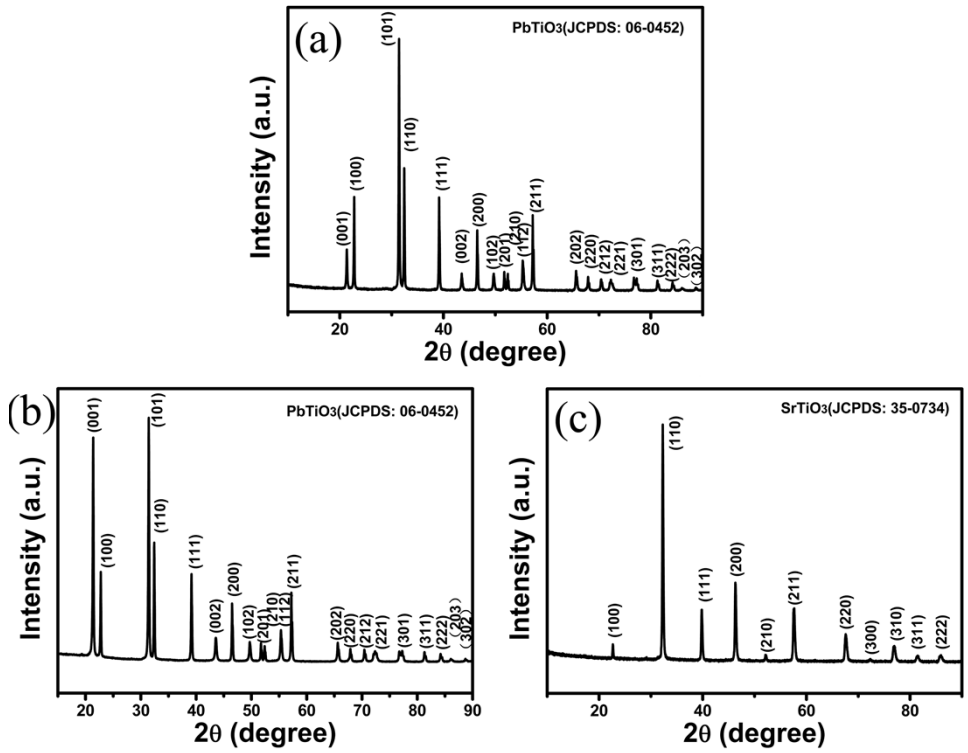

Fig.S6 XRD patterns of the hydrothermal-sintering synthesized perovskite $PbTiO_3$ nanofibers, hydrothermally-synthesized $PbTiO_3$ nanoplates and $SrTiO_3$ nanoparticles.

Fig.S6 shows the XRD patterns of the hydrothermal-sintering synthesized perovskite $PbTiO_3$ nanofibers, and hydrothermally-synthesized $PbTiO_3$ nanoplates and $SrTiO_3$ nanoparticles, as displayed in Fig.S6(a), (b) and (c), respectively. Typically, the perovskite $PbTiO_3$ nanofibers were transformed from pre-perovskite $PbTiO_3$ nanofibers via a subsequent 650 ^oC sintering for 1h in air. All the diffraction peaks can be well indexed into the tetragonal perovskite $PbTiO_3$ (JCPDS: 06-0452) in Fig.S6 (a) and (b), and the XRD pattern in Fig. S6(c) matched well with cubic perovskite $SrTiO_3$ (JCPDS: 35-0734).

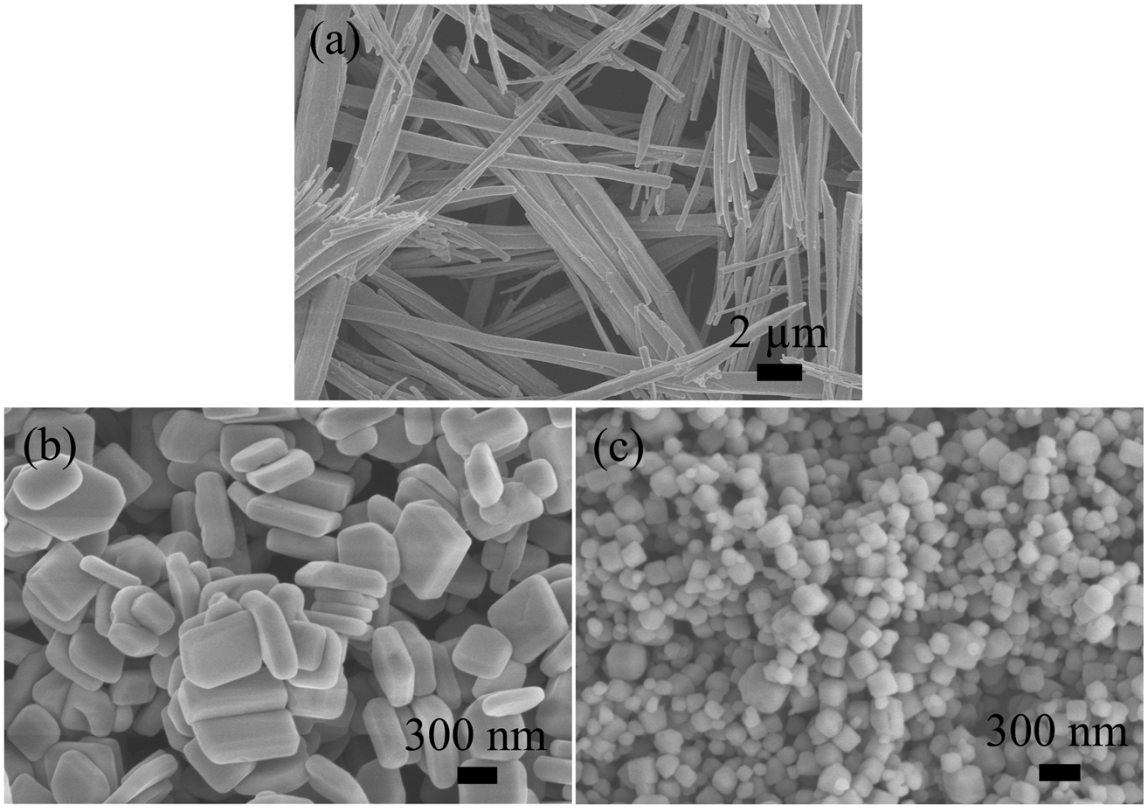

Fig.S7 SEM images of the hydrothermal-sintering synthesized perovskite $PbTiO_3$ nanofibers (a), hydrothermally synthesized $PbTiO_3$ nanoplates(b) and $SrTiO_3$ nanoparticles (c).

Fig.S7 shows the SEM images of the hydrothermal-sintering synthesized perovskite $PbTiO_3$ nanofibers, $PbTiO_3$ nanoplates and $SrTiO_3$ nanoparticles. In Fig. S7 (a), the size of $PbTiO_3$ nanofibers was ~200 nm in diameter and tens of micrometers in length. The $PbTiO_3$ nanoplates were ~700 nm in lateral size and ~100 nm in thickness, as in Fig. S7(b). The $SrTiO_3$ nanoparticles have a size of ~100 nm in Fig. S7(c).

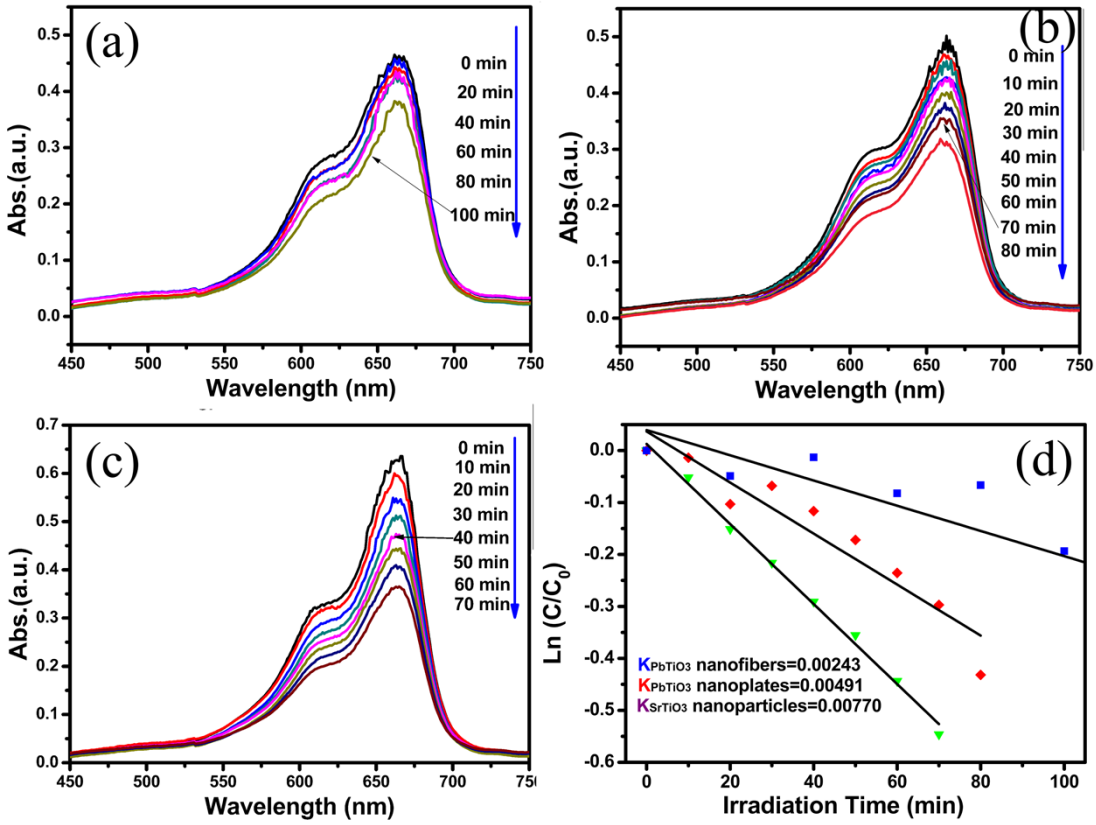

Fig.S8 Absorption changes of MB solution under photocatalytic process: MB degradation with the presence of hydrothermally synthesized (a) $PbTiO_3$ nanofibers, (b) $PbTiO_3$ nanoplates, (c) $SrTO_3$ nanoparticles and (d) corresponding first-order plots for the above materials

As a comparison, we have chosen $PbTiO_3$ nanofibres, nanoplates and $SrTiO_3$ nanoparticles as catalyst materials to explore their photocatalytic activity and performance under visible light irradiation. The photodegradation experimental conditions have been set as previously depicted in *Experimental Section*. Fig. S8 (a)-(c) refers to the detailed absorption spectrum of perovskite $PbTiO_3$ nanofibres, nanoplates and $SrTiO_3$ nanoparticles, respectively. And the corresponding first-order plot for each material has been given in Fig.S8 (d). The calculated k for each catalyst material has been determined to be 0.00243 ($PbTiO_3$ nanofibers), 0.00491 ($PbTiO_3$ nanoplates) and 0.00770 ($SrTiO_3$ nanoparticles), which are all comparable to that of blank experiment (no catalyst), and far less than 0.042 when PT OCT was used as catalyst in the experiment.

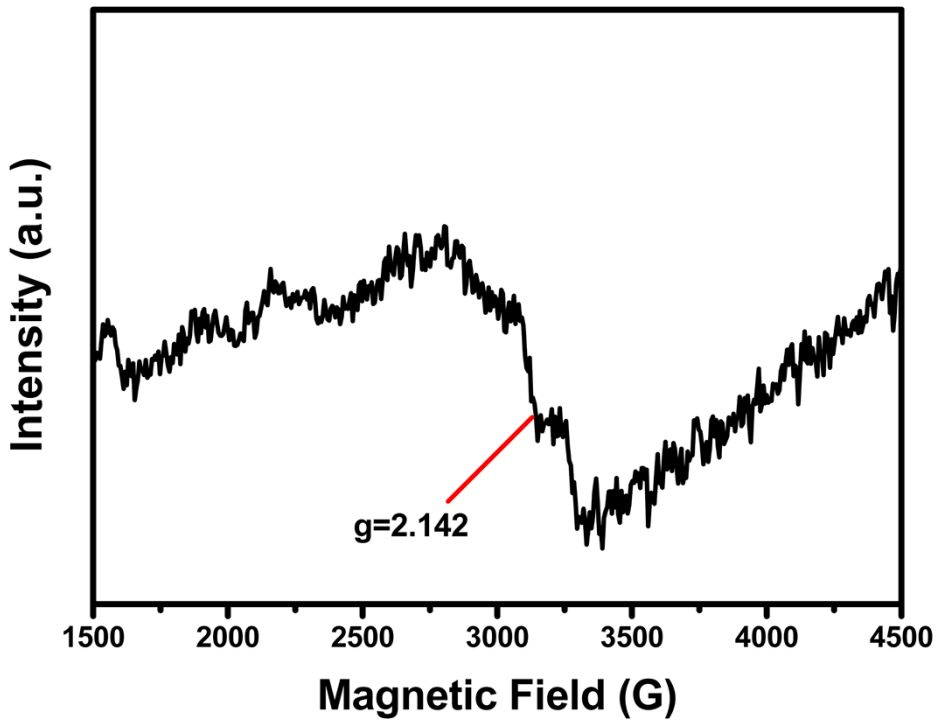

Fig.S9 ESR spectrum of PT OCT nanocrystals at 100K without UV illumination

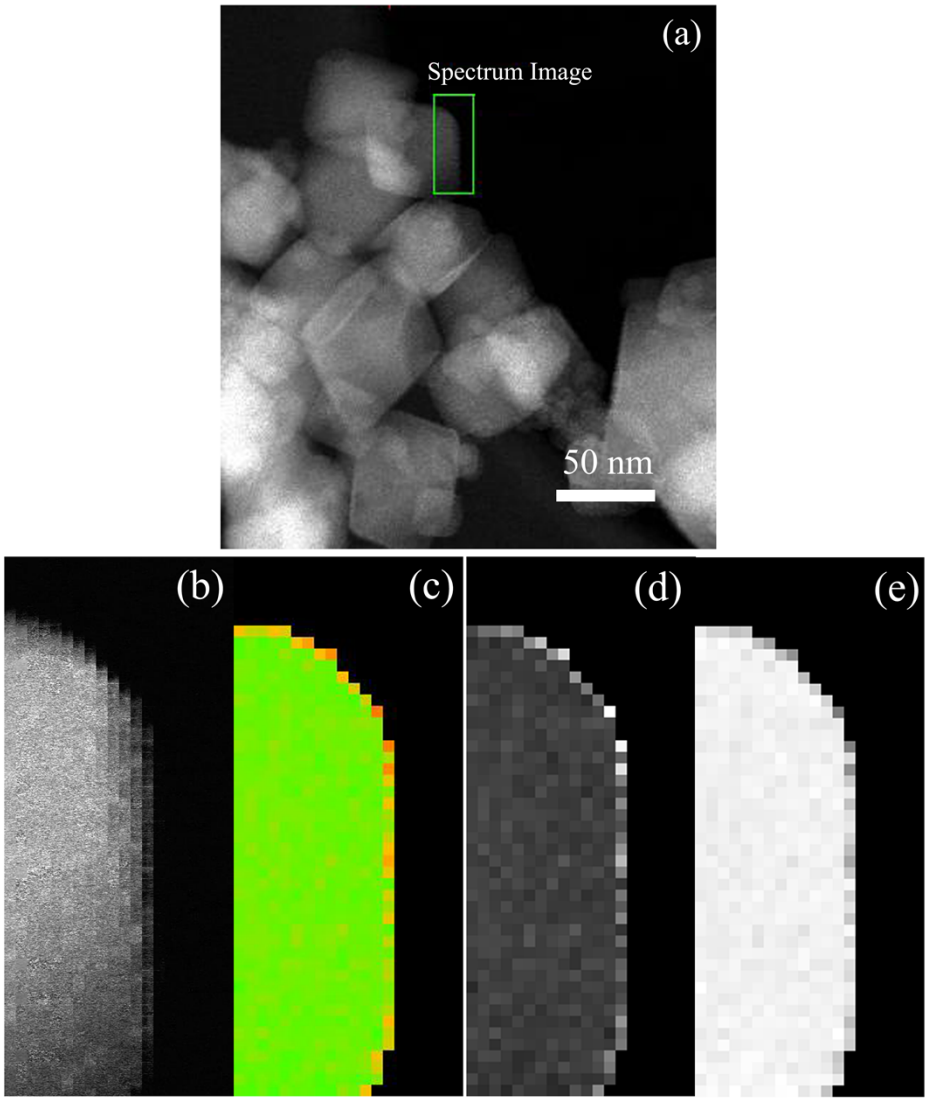

Fig.S10 (a) Dark field STEM image of PT OCT nanocrystals, (b) ADF image of the survey region acquired simultaneously with EELS spectrum, and (c) Color map of concentration (red=Li; green=Ti) and element maps of Li (d) and Ti (e) are obtained with EELS quantifications

STEM Electron Energy Loss Spectroscopy (EELS) mapping and the microscope was operated at 120 kV acceleration voltage to avoid knock-on damage. The convergence angle was 21 mrad and a collection angle of approximately 160 mrad was chosen to maximize the acquisition efficiency. The analysis was performed on the raw data after background subtraction, and no other data pre-treatment was employed.

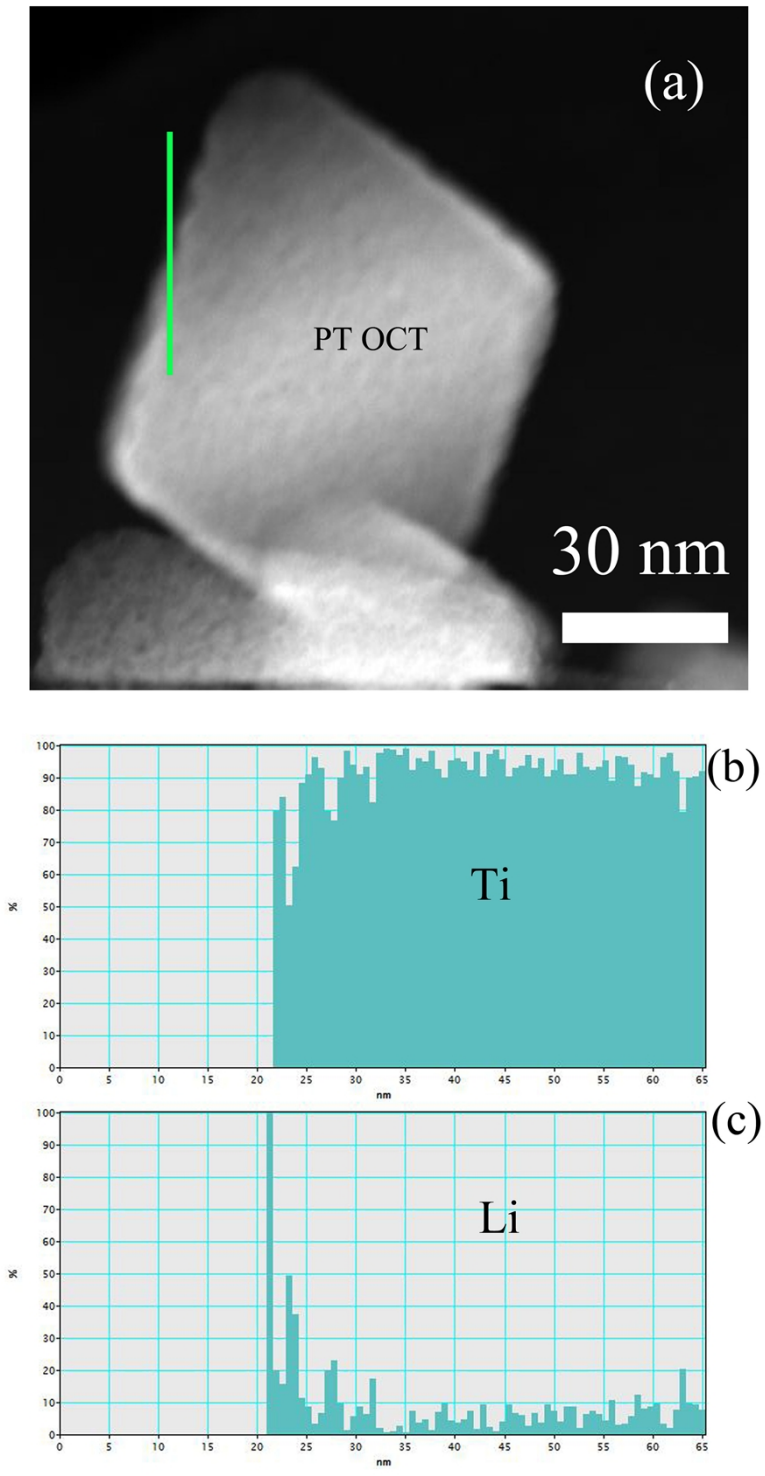

Fig.S11 (a) Dark field STEM image of PT OCT, line scan profile of (b) Ti and (c) Li derived by EELS quantification. Li concentrate surface layer can be observed. In the EELS line scan, each single pixel corresponds to an EELS spectrum, which was quantified to derive a ratio of Ti and Li.

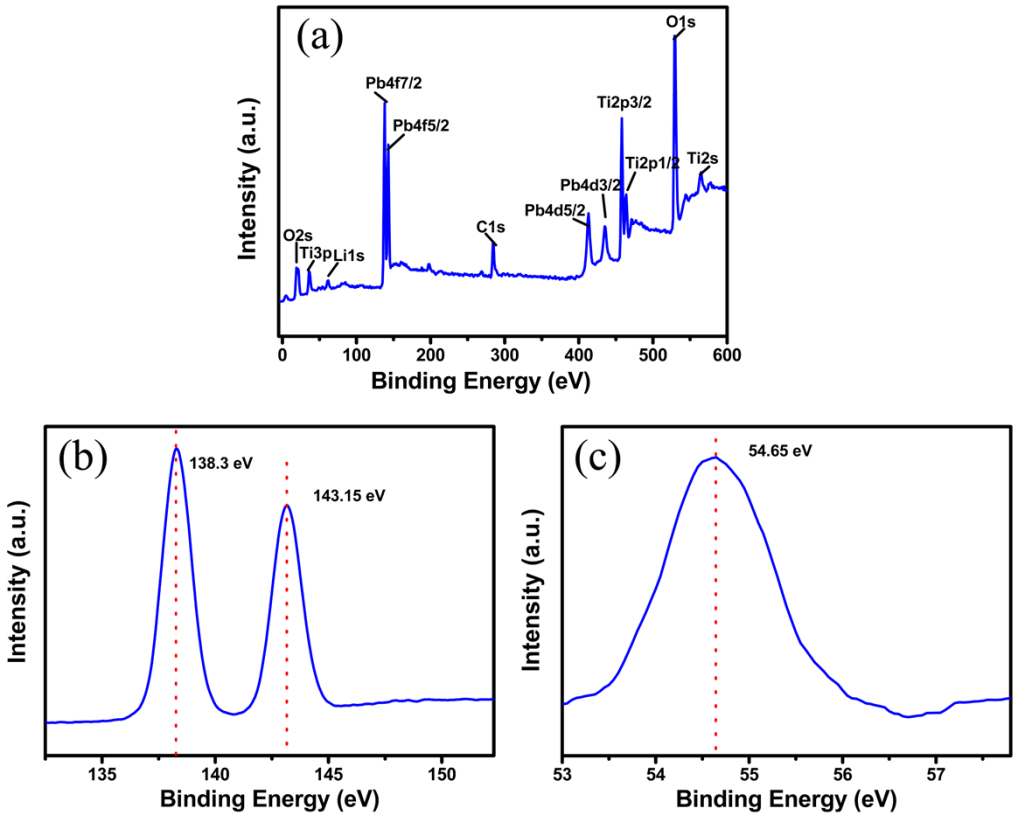

Fig.S12 (a) Survey spectra of PT OCT nanocrystals, XPS spectra of (b) Pb4f and (c) Li1s of PT OCT nanocrystals

X-ray photoelectron spectroscopy (XPS) can be used to investigate the chemical states and the composition of the surface through observation of structure for core electrons. Fig. S12(a) gives the survey XPS spectra of PT OCT in the binding energy range of 0~600 eV, which demonstrates that the surface elements on PT OCT nanocrystals include Pb, Ti, O, Li and no other elements can be detected except for carbon. Fig. S12(b) and (c) present the XPS narrow scan spectra of Pb4f and Li1s core level peaks, respectively. The XPS narrow scan spectrum of Pb4f core level peaks were located at 138.3 eV and 143.15 eV. The Li1s core level peak was located at 54.65 eV, which is very close to the binding energy of Li-O (55±0.5 eV).[3] It can be determined from the XPS result that the as-synthesized PT OCT nanocrystals contain Pb, Ti and O, as well as the formation of Li-O bond on the surface of the product.

Reference

(1) G. Burns and B. A. Scott, *Phys. Rev. Lett.*, 1970, **3**, 167-170.
(2) J. Moon, J. A. Kerchner, J. LeBleu, A. A. Morrone and J. H. Adair, *J. Am. Ceram. Soc.*, 1997, **80**, 2613-2623.
(3) (a) L. M. Suo, Y. S. Hu, H. Li, M. Armand and L. Q. Chen, *Nat. Commun.*, 2013, DOI: 10.1038/ncomms2513. (b) A. Schechter and D. Aurbach, *Langmuir*, 1999, **15**, 3334-3342.